Journal of Biomolecular NMR, **17:** 137–151, 2000.
KLUWER/ESCOM

RFAC, a program for automated NMR R-factor estimation

Wolfram Gronwald[a], Renate Kirchhöfer[a], Adrian Görler[a], Werner Kremer[a], Bernhard Ganslmeier[a], Klaus-Peter Neidig[b] & Hans Robert Kalbitzer[a,*]
[a]*Department of Biophysics and Physical Biochemistry, University of Regensburg, Postfach, D-93040 Regensburg, Germany;* [b]*Bruker Analytik GmbH, Software Department, Rudolf Plank-Str. 23, D-76275 Ettlingen, Germany*

Received 3 January 2000; Accepted 18 April 2000

Key words: automated assignment, protein structure, R-factor

Abstract

A computer program (RFAC) has been developed, which allows the automated estimation of residual indices (R-factors) for protein NMR structures and gives a reliable measure for the quality of the structures. The R-factor calculation is based on the comparison of experimental and simulated ^{1}H NOESY NMR spectra. The approach comprises an automatic peak picking and a Bayesian analysis of the data, followed by an automated structure based assignment of the NOESY spectra and the calculation of the R-factor. The major difference to previously published R-factor definitions is that we take the non-assigned experimental peaks into account as well. The number and the intensities of the non-assigned signals are an important measure for the quality of an NMR structure. It turns out that for different problems optimally adapted R-factors should be used which are defined in the paper. The program allows to compute a global R-factor, different R-factors for the intra residual NOEs, the inter residual NOEs, sequential NOEs, medium range NOEs and long range NOEs. Furthermore, R-factors can be calculated for various user defined parts of the molecule or it is possible to obtain a residue-by-residue R-factor. Another possibility is to sort the R-factors according to their corresponding distances. The summary of all these different R-factors should allow the user to judge the structure in detail. The new program has been successfully tested on two medium sized proteins, the cold shock protein (*Tm*Csp) from *Termotoga maritima* and the histidine containing protein (HPr) from *Staphylococcus carnosus.* A comparison with a previously published R-factor definition shows that our approach is more sensitive to errors in the calculated structure.

*Abbreviations: Tm*Csp, cold shock protein from *Thermotoga Maritima*; HPr, histidine containing phosphocarrier protein; NOE, nuclear Overhauser effect; NOESY, nuclear Overhauser effect spectroscopy; RMSD, root mean square deviation.

Introduction

During the last few years an increasing number of protein NMR structures has been published. So far the quality of an NMR structure is mainly judged by factors such as distance or angle constraint violations, RMSD values of the obtained set of structures and the quality of the Ramachandran plot (for an overview see Laskowski et al., 1998). However, all these methods do not provide a direct measure of how well the obtained structures fit the experimental data. RMSD values, for example, give a measure for the precision of an NMR structure but they are not necessarily a measure for the even more important accuracy. In fact, they can be rather meaningless if the parameters selecting the set of structures to be compared are not defined carefully: a subset with small RMSD values can easily be selected if a sufficiently large number of structures has been calculated. A comparison between experimental and back-calculated NOESY spectra leads to an error function similar to the R-factor used in crystallography (Brünger et al., 1987).

*To whom correspondence should be addressed. E-mail: hans-robert.kalbitzer@biologie.uni-regensburg.de

This NMR R-factor gives a direct value for the quality of the NMR structure obtained. In the literature different definitions for NMR R-factors can be found (Lefevre et al., 1987; Gupta et al., 1988; Brandan et al., 1990; Nikonowicz et al., 1990; Lane, 1990; Baleja et al., 1990; Borgias et al., 1990; Borgias and James, 1990; Bonvin et al., 1991; Gonzalez et al., 1991; Nilges et al., 1991; Thomas et al., 1991; Mertz et al., 1992; Brünger et al., 1993; Clore et al., 1993; Xu et al., 1995; Cullinan et al., 1996). These R-factors are either used to estimate the quality of the final structure obtained or for refinement purposes. To our knowledge, in all of these approaches manually assigned NOESY peaks are compared to their corresponding back calculated counterparts. Therefore, these R-factor calculations are only possible after the time consuming manual assignment of the NOESY spectra has been performed.

However, often it would be useful to estimate the agreement of a structure model with the experimental data independent of the completion of the NOESY assignment. Typical examples could be the selection of a proper starting model for structure based assignment of NOESY spectra or answering the question whether the structure determined by X-ray crystallography applies also in solution.

For that, the R-factor estimation should be performed directly from the experimental spectrum and should be as automated as possible. For such an automation, we can make use of a number of routines already implemented by us in AURELIA (Neidig et al., 1995): two- and three-dimensional NOESY spectra can be back calculated from a given structure on the basis of the complete relaxation matrix formalism (Görler and Kalbitzer, 1997; Görler et al., 1999a), the spectra themselves can be analysed with the automated routines for peak picking (Neidig et al., 1990), peak integration (Geyer et al., 1995), and signal and artefact recognition based on a Bayesian method (Antz et al., 1995; Schulte et al., 1997).

When the assignment of the NOESY spectra is fully automated and based only on the test structure in use, there is no bias caused by the manual assignment in the R-factor calculation. Especially, if there are large structural differences between two structures, it is quite common that for the same experimental signal several different assignments are possible. However, a manual assignment would not automatically change with the current test structure. Therefore, using the automated assignment procedure, structures from different sources can easily be compared to each other and the structure that explains the experimental data best is quickly found. In addition, one can take non-assigned peaks into account as well. These non-assigned peaks are an important measure for the quality of a structure, since it should be possible to explain all experimental peaks using the correct structure.

The automated comparison of the back calculated spectra with the experimental spectra opens an avenue to define different NMR R-factors tuned to the problem under investigation as it is already routine in X-ray crystallography. To give the user a more detailed picture about the quality of a structure, a series of different R-factors can be developed, like a global R-factor, different R-factors for the intra residual NOEs, the inter residual NOEs, sequential NOEs, medium range NOEs and long range NOEs. Furthermore, R-factors can be calculated for various user defined parts of the molecule or it is possible to obtain a residue-by-residue R-factor. Another possibility is to calculate separate R-factors for various distance classes. The summary of all these different R-factors should allow the user to judge the structure in detail.

To test the program RFAC two medium sized proteins, the cold shock protein (*Tm*Csp) from *Thermotoga maritima* and the histidine containing Protein (HPr) from *Staphylococcus carnosus*, were used. *Tm*Csp is 66 residues in size and its tertiary structure is formed by a five stranded β-barrel and one α-helical turn (Harrieder, 1998; Kremer et al., to be published). HPr is 88 residues in size and its structure consists of three α-helices and a four stranded anti parallel β-sheet (Görler et al., 1999b).

Materials and methods

NMR-samples

The spectra used were recorded from a sample from 1.5 mM Csp from *Thermotoga maritima* in 92% H_2O/8% D_2O (v/v), pH 6.5 and a sample from 4.3 mM HPr from *Staphylococcus carnosus* in 90% H_2O/10% D_2O (v/v), pH 7.2.

NMR spectroscopy

The NMR spectra were measured on a Bruker DMX-800 spectrometer operating at proton frequencies of 800 MHz. NOESY spectra (Jeener et al., 1979) were recorded with mixing times of 160 ms and 150 ms for *Tm*Csp and HPr, respectively. Phase-sensitive detection in the t_1-direction was obtained using time-

proportional phase increments (TPPI; Marion and Wüthrich, 1983). Spectra were recorded at 303 K and 298 K, respectively. The time domain data set of *Tm*Csp consisted of 512 real data points in the t_1-direction and 2048 complex data points in the t_2-direction. Data were multiplied by a Gaussian filter (Ferrige and Lindon, 1978) and baseline-corrected with the routines contained in the program XWIN-NMR (Bruker). The final size of the real part of the spectrum was 1024 × 2048 data-points. The time domain data set of HPr consisted of 1024 real data points in the t_1-direction and 4096 complex data points in the t_2-direction. The HPr data were filtered and baseline-corrected as the *Tm*CSP data. The final size of the real part of the spectrum was 1024 × 4096 data points. The sequential assignments for HPr from *S. carnosus* were taken from Beneicke (1994) and Görler (1998), the sequential assignments of *Tm*Csp were taken from Harrieder (1998).

Software

The NMR data were processed with the program XWINNMR (Bruker). Peak picking, integration, Bayesian analysis, back calculation of NOESY spectra, and data inspection were performed with the program AURELIA (Bruker). Automated assignment of the NOESY spectra was done with the program NOEASSIGN (Görler et al., to be published). The different R-factor definitions are combined into an easy to use program (RFAC) which is started from the command line and will either run in a UNIX or PC environment. It is written in standard ANSI C and can be obtained from the authors. It will also be implemented in the graphical environment of a new program part (AUREMOL) of AURELIA under development which is aimed to the automated structure determination of biological macromolecules.

Theoretical considerations and algorithms

The automated R-factor analysis envisaged here consists in principle of two separate parts: (1) the comparison of the experimental NOESY spectrum with the NOESY spectrum back calculated from a given structure and (2) the calculation of the R-factor(s) from the data. In the first part the NOESY spectrum has to be calculated from a structure using the sequential assignments; that is, a three-dimensional structure must be available and the spin systems have to be assigned completely or almost completely. Optimally, the back calculation of the NOESY spectrum is performed on the basis of the complete relaxation matrix analysis. In our implementation we use the program RELAX (Görler and Kalbitzer, 1997) which gives a list of back calculated peaks (*B*-list) defined by their positions and intensities (volumes). The experimental two-dimensional NOESY spectrum is automatically peak picked and integrated. In addition, the probabilities p_i of the peaks i to be true NMR signals and not noise or artefact peaks are calculated according to Bayes' theorem with AURELIA. The probability values p_i provide a measure how reliable the peaks i are, their definition has been described previously (Antz et al., 1995; Schulte et al., 1997). They are used as weighting factors during the calculation of the R-factors. The AURELIA output then consists of the peak positions connected with a list of volumes V_i and a list containing the probability values p_i. This output is merged to the list of unassigned experimental peaks called *U*-list. This *U*-list is compared with the *B*-list and automatically assigned using the assignment program NOEASSIGN (Görler, 1998; Görler et al., to be published) which is part of the RELAX package. Basically the program tries first to optimally adapt the chemical shift values obtained from the general sequential resonance assignment to the actual experimental data by a global comparison of the back calculated spectrum with the experimental spectrum. The peak assignment itself is done on local peak clusters. For each back calculated peak a search is performed if a corresponding experimental peak exists in a given search radius (usually 0.01 ppm). If more than one solution exists the decision is made based on a maximum likelihood criterion. The resulting list of assigned experimental peaks is called the *A*-list. The *U*-, *B*- and *A*-list are fed into the program RFAC. Here the *U*-list can be further reduced by applying a lattice algorithm which can be used if one assumes that the sequential assignment is true and almost complete. In this algorithm only non-assigned peaks are taken into account where at least one back calculated peak in each dimension can be found within a distance of 0.01 ppm. In this context it is important to note that for each atom at least the structure independent diagonal peak is back calculated. In cases where more than one back calculated peak is assigned to a single experimental peak, the mean volume of the corresponding back calculated peaks is estimated before the comparison is done while the volume of the experimental peak is divided by the number of corresponding back calculated peaks.

In general, the R-factor (residual index) should measure the agreement between the experimental data set and the data back calculated from the structure. In its simplest form it is defined by

$$R_1 = \frac{\sum_{i \in A} \left| I_{\mathrm{exp},i} - sf \cdot I_{\mathrm{calc},i} \right|}{\sum_{i \in A} \left| I_{\mathrm{exp},i} \right|} \tag{1}$$

and the summation is performed over the data points i with intensities I_i in a given set A. With this definition R is 0 if the agreement is perfect and > 0 for all other cases. In NMR spectroscopy and X-ray crystallography one has to normalise the experimental data (or the calculated data) since the experimental values are scaled by a constant factor depending on not exactly known instrumental and experimental parameters. The optimal scale factor is found when the likelihood function *L(sf)* adopts its maximum value.

$$L(sf) = \prod_{i \in A} p \cdot (sf \cdot I_{\mathrm{calc},i}, I_{\mathrm{exp},i}) \tag{2}$$

Here, p is the probability that for a calculated value $sf \cdot I_{\mathrm{calc},i}$ the value $I_{\mathrm{exp},i}$ is measured. From Equation 2 follows for the scale factor *sf* (Görler, 1998)

$$sf = \frac{\sum_{i \in A} I_{\mathrm{exp},i} \cdot I_{\mathrm{calc},i}}{\sum_{i \in A} I^2_{\mathrm{calc},i}} \tag{3}$$

The above definition of the R-factor is well suited for X-ray crystallography but for NMR spectroscopy several difficulties arise: the exact positions of the X-ray reflections are determined by the crystal lattice and exactly known. Therefore, the assignments of the reflection spots are usually unambiguous and only the intensities of these spots determine the R-factor. The data set A corresponding to a given resolution can easily be assigned and used for the calculation of the R-factor (which is always dependent on A). In NMR spectroscopy many assignments of experimental peaks are ambiguous and many experimental peaks are artefacts. Therefore, in literature only the set A of manually assigned peaks is used for the calculation of the R-factor. By application of Equation 1 to NOESY spectra one can define a measure for the error (Equation 4) that corresponds to a normalised mean deviation (Gonzalez et al., 1991). Please note that in the following for all R-factor calculations the intensities will be replaced by their corresponding volumes *V*.

$$R_2 = \sqrt{\frac{\sum_{i \in A} (V_{\mathrm{exp},i} - sf \cdot V_{\mathrm{calc},i})^2}{\sum_{i \in A} V^2_{\mathrm{exp},i}}} \tag{4}$$

Since, unlike in X-ray crystallography, the set of peaks is incomplete and dominated by the (structurally less important) strong short range NOEs, R is dominated also by the volumes of these 'trivial' peaks. Therefore, usually V is replaced by a more meaningful function *f(V)* which emphasises the more important long range NOEs. The most common form of *f(V)* is

$$f(V) = V^{\alpha} \tag{5}$$

Thus a more general form of R_2 is then given by

$$R_2(\alpha) = \sqrt{\frac{\sum_{i \in A} (V^{\alpha}_{\mathrm{exp},i} - sf_{\alpha} \cdot V^{\alpha}_{\mathrm{calc},i})^2}{\sum_{i \in A} V^{2\alpha}_{\mathrm{exp},i}}} \tag{6}$$

If a *f(V)* as described in Equation 5 is used the calculation of the scale factor must be changed accordingly.

$$sf_{\alpha} = \frac{\sum_{i \in A} (V_{\mathrm{exp},i} \cdot V_{\mathrm{calc},i})^{\alpha}}{\sum_{i \in A} V^{2\alpha}_{\mathrm{calc},i}} \tag{7}$$

As relation (2) this expression fulfills the important condition that it gives the correct value of *sf* in the error free case where all experimental and back calculated peak volumes differ only by a proportionality factor. With $\alpha = -1/6$, $f(V)$ is in first order proportional to the inter nuclear distance and one obtains the distance related R already defined by Gonzales et al. (1991).

In the automated R-factor calculation no user interferes who decides (1) which peak in the NOESY spectrum is a true resonance and (2) if an assignment of a cross peak is correct. In principle only probabilities $p_{\mathrm{exp},i}$ and $p_{\mathrm{calc},i}$ exist for cases (1) and (2), respectively. A method for estimating $p_{\mathrm{exp},i}$ has already been developed, an algorithm does not yet exist for estimating $p_{\mathrm{calc},i}$. Consequently, in the following we will explicitly make use only of the probabilities $p_{\mathrm{exp},i}$. With these probabilities Equations 4 and 6 can be rewritten as

$$R_3(\alpha) = \sqrt{\frac{\sum_{i \in A} (V^{\alpha}_{\mathrm{exp},i} - sf_{\alpha} \cdot V^{\alpha}_{\mathrm{calc},i})^2 \cdot p^2_{\mathrm{exp},i}}{\sum_{i \in A} V^{2\alpha}_{\mathrm{exp},i} \cdot p^2_{\mathrm{exp},i}}} \tag{8}$$

The above R-factors only estimate how well the assigned peaks are explained by the structural model but

they do not provide a direct measure for the quality of the structure. For doing this the R-factor should decrease if more peaks are assigned correctly and explained by the structural model. A practical expansion of Equation 8, including the non-assigned peaks can be defined by

$$R_4(\alpha) = \sqrt{\frac{\sum_{i\in A}(V^{\alpha}_{\mathrm{exp},i} - sf_{\alpha}\cdot V^{\alpha}_{\mathrm{calc},i})^2\cdot p^2_{\mathrm{exp},i} + \sum_{i\in U}(V^{\alpha}_{\mathrm{exp},i} - sf_{\alpha}\cdot V^{\alpha}_{\mathrm{noise}})^2\cdot p^2_{\mathrm{exp},i}}{\sum_{i\in A} V^{2\alpha}_{\mathrm{exp},i}\cdot p^2_{\mathrm{exp},i} + \sum_{i\in U} V^{2\alpha}_{\mathrm{exp},i}\cdot p^2_{\mathrm{exp},i}}} \quad (9)$$

The first summation is performed over all assigned experimental peaks contained in the *A*-list (set *A*) and the second summation is performed over the list of unassigned peaks *U* (set *U*). $V_{\mathrm{calc},i}$ are the corresponding calculated intensities (volumes). For set *U* the logic extension of R_3 would assign the strongest back calculated cross peak with suitable coordinates as $V_{\mathrm{calc},i}$. However, since for $\alpha = -1/6$ very small volumes in R_4 dominate the R-value, more stable results can be expected in this case if a lower limit is set for $V_{\mathrm{calc},i}$. It is computationally efficient to set $V_{\mathrm{calc},i}$ to a value which just cannot be detected safely in the experimental spectrum, that is, to the intensity V_{noise} of a standard noise peak. In the present implementation, it is possible to calculate the noise intensity automatically or a user specified noise intensity can be used. If the noise volume is calculated by the program the weakest back calculated intensity where the corresponding distance is not greater than the detection limit is selected. In the automatic routine a detection limit of 0.5 nm is assumed. Since in R_4 ($\alpha = -1/6$) the large distances (small volumes) dominate the expression, the above normalisation of the R-factor leads to a strong dependence on the exact value of the V_{noise} term. This influence can be diminished by inclusion of V_{noise} in the denominator:

$$R_5(\alpha) = \sqrt{\frac{\sum_{i\in A}(V^{\alpha}_{\mathrm{exp},i} - sf_{\alpha}\cdot V^{\alpha}_{\mathrm{calc},i})^2\cdot p^2_{\mathrm{exp},i} + \sum_{i\in U}(V^{\alpha}_{\mathrm{exp},i} - sf_{\alpha}\cdot V^{\alpha}_{\mathrm{noise}})^2\cdot p^2_{\mathrm{exp},i}}{\sum_{i\in A} V^{2\alpha}_{\mathrm{exp},i}\cdot p^2_{\mathrm{exp},i} + \sum_{i\in U}(V^{\alpha}_{\mathrm{exp},i} - sf_{\alpha}\cdot V^{\alpha}_{\mathrm{noise}})^2\cdot p^2_{\mathrm{exp},i}}} \quad (10)$$

In case of $\alpha = 1$ the standard noise intensity V_{noise} for the R-factors R_4 and R_5 can be set to 0, since strong unassigned signals will lead to increasing R-factors in this equation. With this definition the two R-factors in Equations 9 and 10 become equal.

The R-factors $R_{4,5}$ indicate how well the experimental signals are explained by back calculated peaks. However, one can also define an R-factor to check how well the back calculated signals are explained by experimental data. A definition analogous to R_5 uses the non-assigned back calculated signals instead of the non-assigned experimental peaks:

$$R_6(\alpha) = \sqrt{\frac{\sum_{i\in A}(V^{\alpha}_{\mathrm{exp},i} - sf_{\alpha}\cdot V^{\alpha}_{\mathrm{calc},i})^2\cdot p^2_{\mathrm{exp},i} + \sum_{i\in U'}(V^{\alpha}_{\mathrm{noise}} - sf_{\alpha}\cdot V^{\alpha}_{\mathrm{calc},i})^2\cdot p^2_{\mathrm{exp},i}}{\sum_{i\in A} V^{2\alpha}_{\mathrm{exp},i}\cdot p^2_{\mathrm{exp},i} + \sum_{i\in U'}(V^{\alpha}_{\mathrm{noise}}\cdot p^2_{\mathrm{exp},i} - sf_{\alpha}\cdot V^{\alpha}_{\mathrm{calc},i})^2\cdot p^2_{\mathrm{exp},i}}} \quad (11)$$

The summation of the unassigned calculated peaks has now to be performed over a different set U′ which contains all back calculated non-assigned peaks with volumes $V_{\mathrm{calc},i} \geq V_{\mathrm{noise}}$.

Instead of the standard noise intensity used in R_4 and R_5 one can assign specific volumes to all experimental peaks which could not be assigned unambiguously by our standard assignment routine. In this way, a new R-factor (R_7) can be defined by using Equation 8 but performing the summation over all experimental peaks. The majority of peaks which are contained in set *U* are originally not assigned since the back calculation from the test structure has not produced a corresponding peak with sufficient intensity. In the first step an assignment for the so far not assigned signals is done solely on chemical shifts without use of any structural information. Artefact and noise peaks are mainly excluded by the use of the lattice algorithm and by using only non-assigned experimental peaks with a high peak probability value p_i. If more than one solution is possible the solution with the largest volume is selected. For increasing the computational efficiency the volumes of these weak peaks can be calculated with sufficient accuracy with the initial slope approximation from the distances.

The above defined R-factors are devised primarily for judging global properties. It is further possible to calculate the R-factor for previously specified regions of the molecule of interest. This allows to judge how well for example a given α-helix or β-strand is defined. In this case R_3 seems to be appropriate where only the subset of the assigned peaks *A* is taken into account.

Another possibility using R_3 is to calculate a separate R-factor for each residue. This can be a useful tool for finding miss-assigned residues. A different way to look at R-factors is to sort them by distance. In this case R_3 is used again and signals are sorted by the corresponding distances of the calculated intensities. We have defined 10 classes starting at 0.15 nm and each with a range of 0.05 nm. The separation of

the R-factor in distance classes allows to check if for example NOEs corresponding to short distances are over-proportionally violated. And this in turn could give a hint if the upper and lower bounds in the structure calculation procedure have been correctly defined. This will be further explained in the Results section.

Results

2D ^{1}H-NOESY spectra of HPr and *Tm*Csp measured at 800 MHz were taken for the R-factor calculation. Since the severe overlap in the aliphatic part of the spectra made peak assignment and integration rather prone to errors, only the NH-region (10.6 ppm to 7.3 for *Tm*Csp and 11.3 ppm to 6.2 ppm for HPr) of each spectrum was used giving 842 (*Tm*Csp) and 1048 (HPr) experimental peaks. For *Tm*Csp four different test structures were used. First we took the final NMR structure (original structure), where 920 NOEs, 52 backbone dihedral angles and 29 H-bonds were used in the structure calculations (Kremer et al., 2000). The second structure was a homology model (Welker et al., 1999) that was based on the X-ray and NMR structures of CspB from *Bacillus subtilis* and on the X-ray structure of CspB from *Escherischia coli*. As third structure we took an early NMR structure where only 89 NOEs but all of the dihedral angles and the H-bonds were used. As the fourth structure an energy minimised extended strand was used. For HPr five different test structures were created. The first structure was the final NMR structure determined from 1301 NOEs, 79 backbone coupling constants and 35 H-bonds (Görler et al., 1999b) which had been energy refined by restrained molecular dynamics in water at room temperature (original structure). With this structure 3000, 6000 and 9000 steps of 0.005 ps of unrestrained molecular dynamics simulations in vacuo at room temperature were performed to obtain increasingly disordered structures (MD3000, MD6000 and MD9000 structure). The last test structure for HPr was again an energy minimised extended strand structure.

The most interesting results obtained with the R-factors defined above will be discussed in the following. We will start showing the results obtained using R_5 ($\alpha = -1/6$) and compare it with the simpler R-factor R_3 ($\alpha = -1/6$) which does not use non-assigned signals. Figure 1 shows the overall R-factors for the various test structures of *Tm*Csp and HPr. For the R-factors in the leftmost set of bars in Figure 1A and B long-range and non-assigned NOEs were used using R_5 ($\alpha = -1/6$). The next set of bars shows the R-factors using only long-range but not non-assigned signals. In the same way R-factors for the intra-residual and non-assigned, intra-residual, sequential and non-assigned, sequential, medium-range and non-assigned, medium-range, all inter-residual and non-assigned and all inter-residual signals were obtained. Medium-range signals are defined as inter-residual signals which are arising from amino acids i and j which are not further apart in the sequence than 4 residues ($i < j$, $j - i \leq 4$). Long range signals are defined as the remaining inter-residual signals. As can be easily seen, the R-factors in the leftmost set of bars are the most discriminating ones with values ranging from 0.9 to 0.4. This is true for both sets of test structures. In case of a less defined structure like an extended strand almost no medium or long-range NOEs are simulated and therefore all experimental peaks which correspond to a medium or long range NOE remain unassigned. The resulting R-factor R_5 ($\alpha = -1/6$) is in this case mostly influenced by the unassigned peaks and is approaching a value of one, while for a good structure only few non-assigned signals remain and the R-factor is dominated by the differences between assigned experimental and calculated signals. Since long-range NOEs are the most sensitive to variations in the three-dimensional structure it can be expected that the most discriminating overall R-factor is obtained if for R_5 ($\alpha = -1/6$) only these are used. The results presented in Figure 1 confirm this expectation. The R-factors obtained with other subsets of assigned peaks are less structure dependent (Figure 1). For the *Tm*Csp test structures a large difference exists between the extended strand and the structure where only a few NOEs were used for the structure calculation. This is due to the fact that the latter structure already possesses the correct fold; therefore the R-factor drops considerably. The intra-residual NOEs without non-assigned signals are not that useful to discriminate correct from incorrect structures, since a lot of distances within a residue are more or less fixed by the geometry of the amino acid. The R-factors for the sequential NOEs alone are more discriminating since most sequential NOEs are strongly dependent on the secondary structure. For *Tm*Csp the second, third and fourth structure all possess the correct fold so that there are only small differences in the R-factors for the sequential NOEs. Since the secondary structure elements of *Tm*Csp are mostly β-strands which are in some regards similar to an extended strand, the difference between the extended strand and the other test

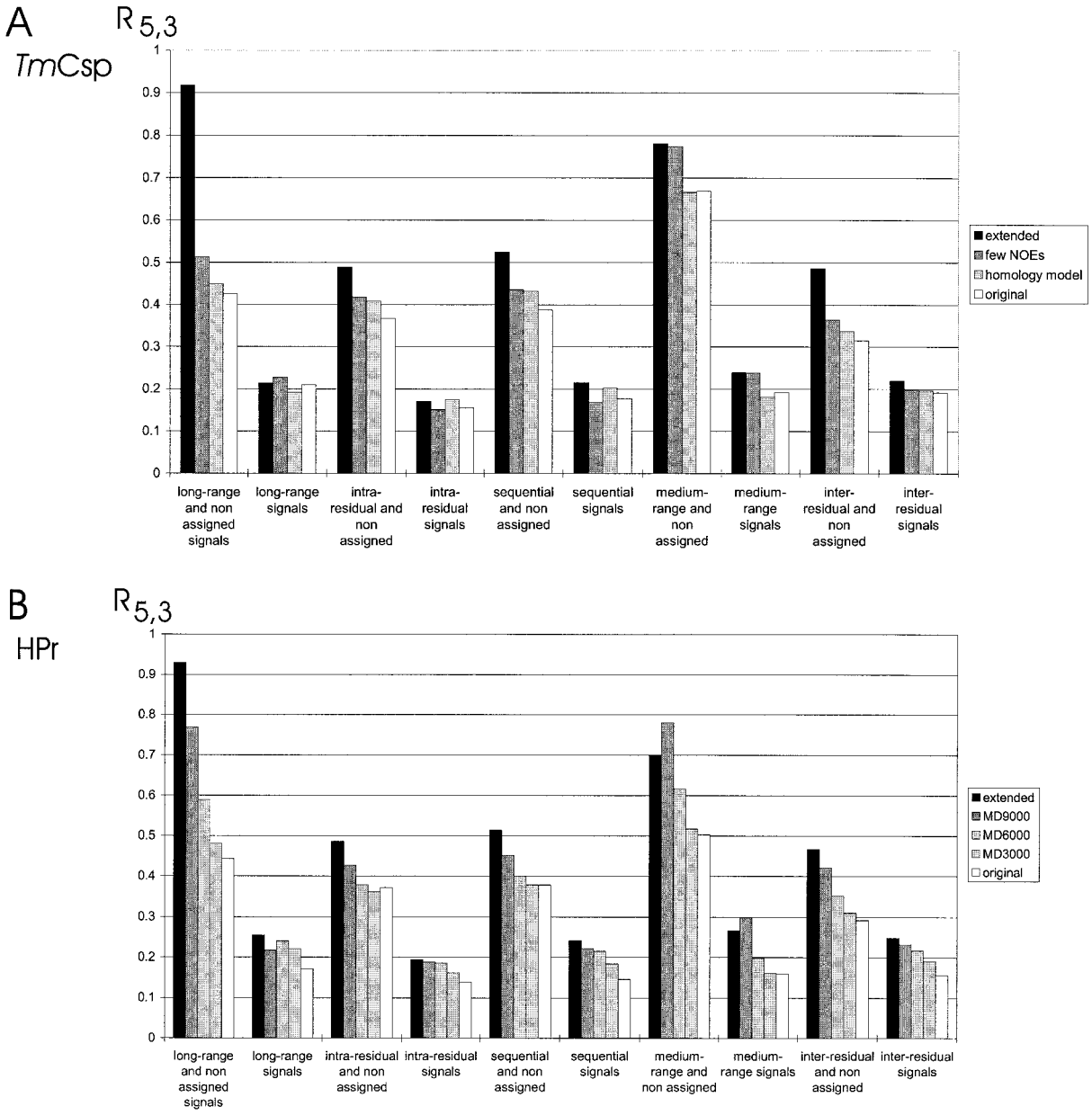

Figure 1. Overall R-factors for *Tm*Csp and HPr. A set of four and five different test structures was used for *Tm*Csp and HPr, respectively. The leftmost set of bars was calculated using R_5 ($\alpha = -1/6$). From the assigned experimental signals only the long-range signals together with all non assigned signals were used. For the original structure of *Tm*Csp 282 out of a total of 842 peaks remained non assigned; this number was further reduced by the lattice algorithm to 148 non assigned peaks. For the extended strand 420 peaks remained non assigned, which were reduced by the lattice algorithm to 286 peaks. Similar results were obtained for the original structure of HPr where 244 of the 1048 experimental peaks remained non assigned, which were reduced by the lattice algorithm to 156 peaks. For the extended strand 444 peaks remained non assigned, which were further reduced to 355 peaks. The next set of bars was calculated using R_3 ($\alpha = -1/6$) and only the long-range NOEs. In the same manner R-factors were calculated using all intra-residual and non assigned, all intra-residual, all sequential and non assigned, all sequential, all medium-range and non assigned, all inter-residual and non assigned and all inter-residual signals. Whenever non assigned signals were included R_5 was used; otherwise R_3 was used.

structures is not very large. For HPr, which possesses a higher helical content, the differences between the various test structures are larger since the secondary structure elements start to unfold during the room temperature MD simulations.

Similar trends as described for the sequential NOEs alone can be observed for the medium- and long-range signals without non-assigned NOEs in Figure 1. This is true for both HPr and *Tm*Csp. For the long-range signals alone it is important to note that for the less well defined structures only very few long range signals have been back calculated and therefore only few experimental signals could be assigned to long-range NOEs. The resulting long-range R-factors are then based only on a few NOEs. This explains the relatively low long-range R-factors for the extended strand structures. For the inter-residual signals of HPr a clear trend is visible with a decreasing R-factor from the extended strand test structures towards the original structures. The results in Figure 1 show that with the inclusion of the non-assigned NOEs the R-factors become generally more discriminating. This demonstrates clearly the importance of the non-assigned NOEs for the R-factor. In the following, we will use the long-range NOEs if not stated otherwise. This selection does not affect the non-assigned peaks since it is not known to which type one particular non-assigned NOE belongs. In case of a good structure the R-factor R_5 ($\alpha = -1/6$) adopts in our test cases values of around 0.4.

Figure 2 shows R-factors using R_3 ($\alpha = -1/6$) for the various secondary structure elements of *Tm*Csp and HPr. In this case only sequential NOEs were used. First, there are generally no long- or medium-range NOEs within secondary structure elements like β-strands. Second, sequential NOEs are more dependent on the secondary structure than intra-residual NOEs. These R-factors should indicate how well one particular secondary structure element is defined. For *Tm*Csp and HPr the original structures give in most cases the lowest R-factors, indicating that there the secondary structure elements are best defined. This is particularly clear for the α-helices and β-strands of HPr.

In Figure 3 separate R-factors were calculated for each residue using R_3 ($\alpha = -1/6$). In this case only the inter-residual NOEs were used, while the intra-residual NOEs were omitted, since they are less structure dependent. It was not possible to use the long-range NOEs alone since for several residues no long-range NOEs were found. To make Figure 3 easier to read, for both *Tm*Csp and HPr only data using the original structure or the extended strand are shown. For *Tm*Csp the R-factors show no large variations for both the extended strand and the original structure. Only for the extended strand structure two dips are visible around residues 30 and 62. In general the values for the extended strand structure are higher than those for the original structure. Much more interesting are the data obtained for HPr. At the N- and C-termini of HPr large R-values are obtained for both the extended strand and the original structure. Since these large R-factors are obtained for the extended strand and for the original structure they seem to be structure independent. A possible explanation can be highly flexible ends. This high flexibility could lead to large differences between observed and back calculated NOEs since for the back calculation only one general correlation time was assumed. Therefore, it might be possible to use R-factors to investigate the dynamics of proteins.

Another way to look at R-factors is to sort them into distance classes. For Figure 4 R-factors were calculated using R_3 ($\alpha = -1/6$) and grouped into 8 distance classes starting at 0.15 nm. Each class had a width of 0.05 nm. The corresponding distances were obtained from the test structures. R-factors were calculated using all inter-residual NOEs. Intra-residual NOEs were excluded from the calculations since they are less dependent on structural changes. To make Figure 4 easier to read a polynomial smoothing was applied to the data. For most of the test structures of *Tm*Csp and HPr low R-factors were obtained for distances in the range between 0.25 nm and 0.5 nm. For larger and shorter distances the R-factors increased. However, there is one exception, that is the homology model of *Tm*Csp. In this case there is almost no distance dependency for the R-factor. It should be noted that the homology model is based on an X-ray structure, while the other folded structures are NMR structures. A possible explanation for the behaviour of the NMR test cases could be that the upper bounds that were applied to very strong NOEs during the structure calculations were too large. This could lead to high R-values, specially for short distances. For large distances above 0.5 nm the R-factors for the NMR test case are increasing again. This could indicate that not enough long-range NOEs are defined for a perfect definition of the tertiary structure, since most of the long range NOEs correspond to larger distances. If the corresponding upper bounds are linearly increasing with the NOE distance this could explain the increasing R-factors for larger distances. If one compares

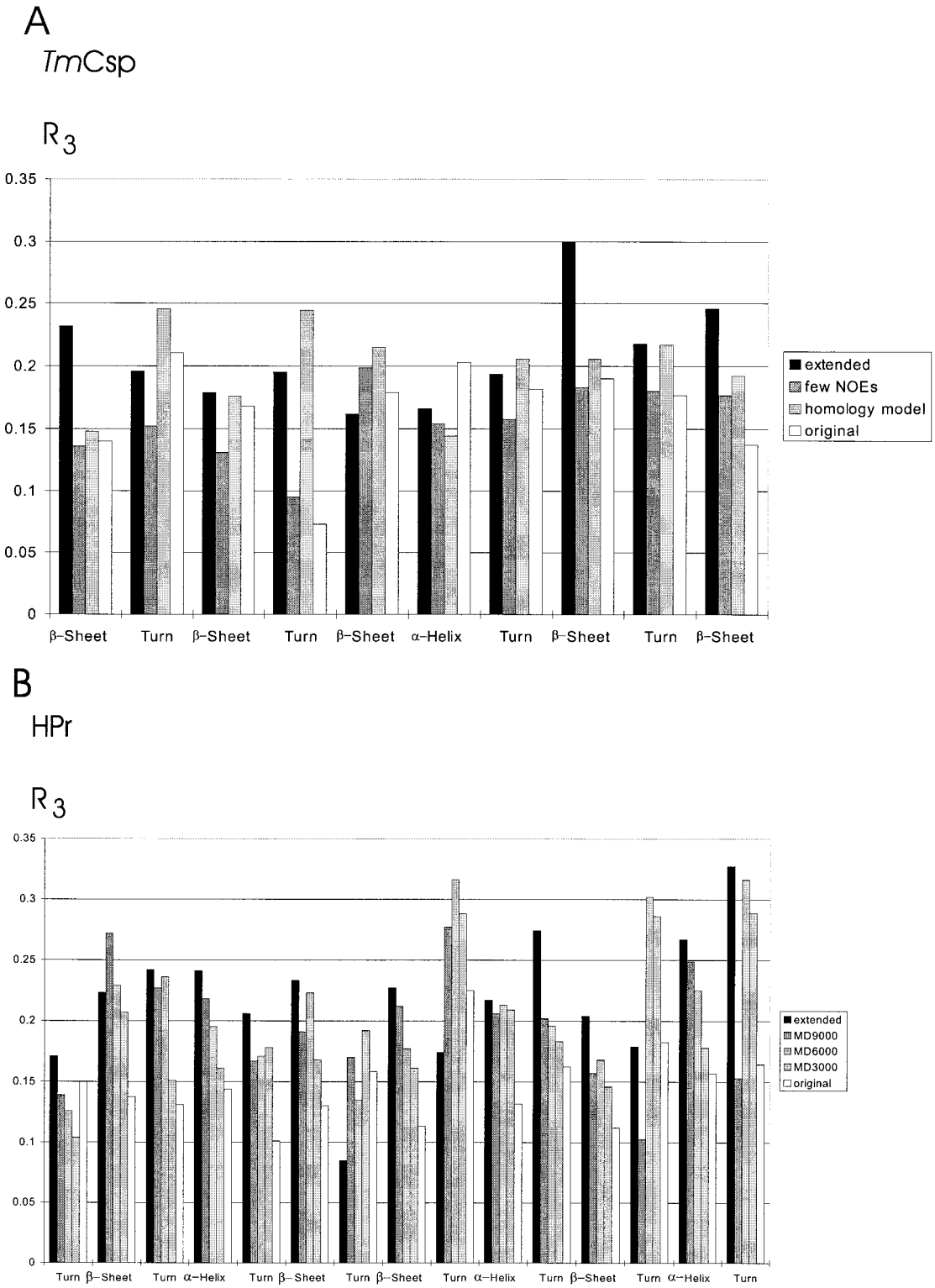

Figure 2. Secondary structure dependent R-factors for *Tm*Csp and HPr. R-factors were calculated according to R_3 ($\alpha = -1/6$) using only the sequential NOEs within a specified secondary structure element.

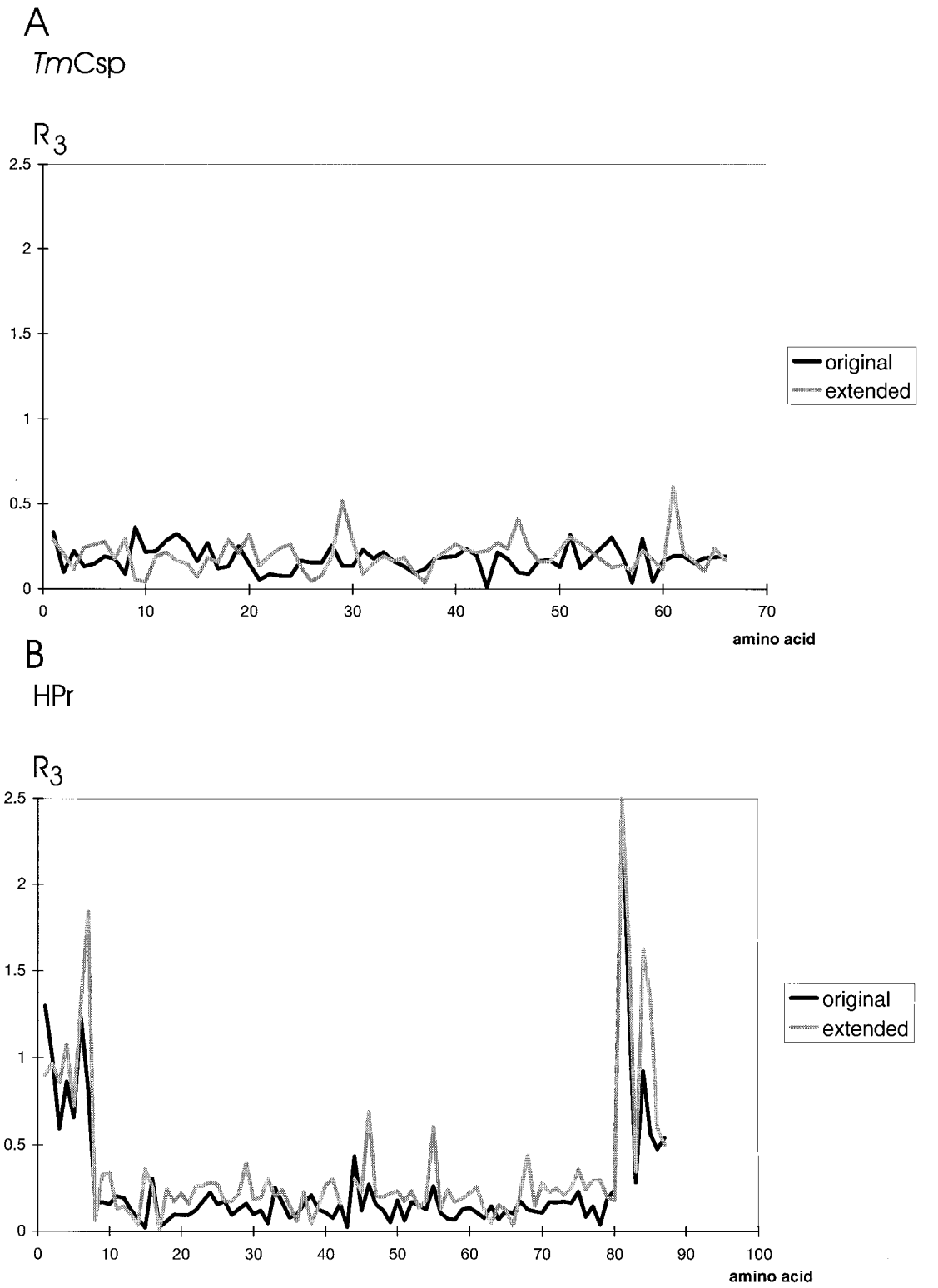

Figure 3. Sequence dependent R-factors for *Tm*Csp and HPr. R-factors are calculated according to R_3 ($\alpha = -1/6$) using all inter-residual NOEs for each residue.

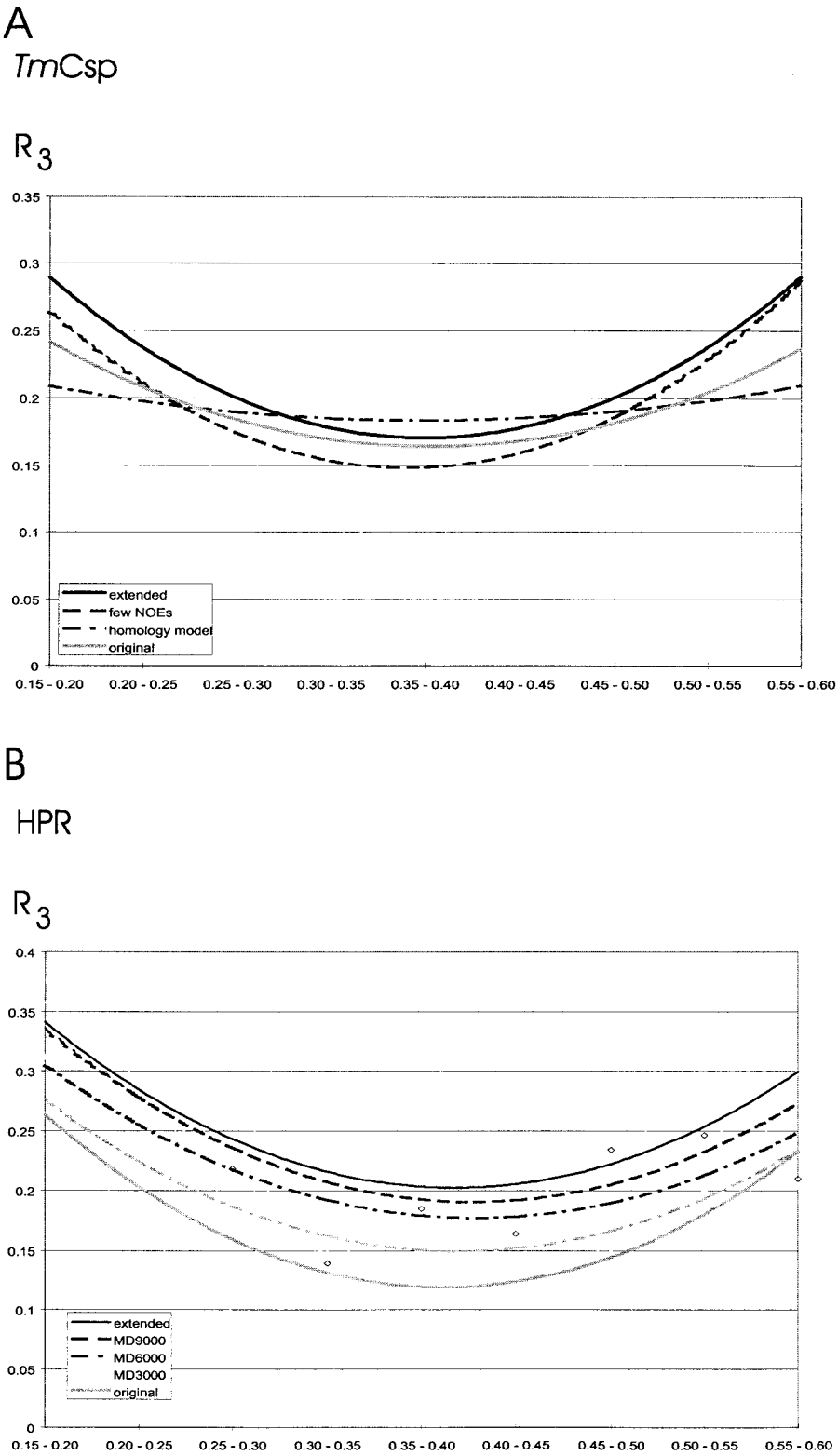

Figure 4. Distance dependent R-factors for *Tm*Csp and HPr. A polynomial smoothing of second order was applied to the data to enhance the readability of the figure. R-factors are calculated according to R_3 ($\alpha = -1/6$) using only the inter-residual NOEs.

for *Tm*Csp the R-factors of the original structure with the R-factors of the 'few NOE' structure one can see that especially for larger distances the R-factors of the original structure are superior.

Table 1 displays the results using a standard R-factor definition (R_2 ($\alpha = -1/6$)) that has been previously defined by Gonzalez et al. (1991). Please note that all assigned signals were used and that they were all weighted equally. Using R_5 ($\alpha = -1/6$) in the HPr test case we had a range in R-factors from 0.97 to 0.44 between the worst and best structure. In comparison, the R-factors obtained using R_2 ($\alpha = -1/6$) for HPr only showed a range from 0.23 to 0.16. For *Tm*Csp the dispersion in R-factors using R_2 ($\alpha = -1/6$) is even lower than for HPr. The main reason for this behaviour is that R_2 ($\alpha = -1/6$) does not take the unassigned signals into account.

So far intensities have been converted into distance-like quantities by setting α to $-1/6$. If one uses the intensities directly ($\alpha = 1$) without conversion into distance-like quantities the R-factor will be dominated by strong NOEs, since a violation of for example 0.05 nm between the ideal and the model structure will have a much larger effect on the R-factor for a NOE corresponding to a short distance than for a NOE corresponding to a large distance. Table 1 shows the corresponding results for *Tm*Csp and HPr using R_4 ($\alpha = 1$). Please note that no standard noise intensity had to be used in this case. As for the other calculations only long-range and non-assigned NOEs were used. Here, no clear correlation between the quality of the structure and the R-factor exists for the four *Tm*Csp test structures. All R-factors are here close to one. For the HPr test cases a correlation between structure and R-factor is visible, although the difference between the best and worst R-factor is only 0.16. Due to the r^{-6} dependency of the NOEs small deviations between the structure present in solution and the test structure will lead to large deviations between simulated and experimental intensities. Since the simulated and experimental intensities themselves are used in R_4 ($\alpha = 1$), a test structure which deviates only a bit from the correct solution structure will get a large R-factor. Only a few strong non-assigned NOEs will further drastically increase the R-factor.

In R_5 the noise volume is also introduced in the denominator. In principle, in the straightforward generalisation of the R-factor to non-assigned peaks (R_4) the noise volume would not occur in the denominator. Table 1 compares the two definitions for *Tm*Csp and shows that R_5 ($\alpha = -1/6$) is more discriminating than R_4 ($\alpha = -1/6$), although the general trends are the same. Again only long-range and non-assigned signals were used. This discrepancy can be rationalised, if one thinks about the worst possible test structure where all experimental peaks remain unassigned. In this case the R-factor using R_5 will approach a value of one. However, if R_4 is used the resulting R-factor will adopt only a value of around 0.5.

The R-factors discussed so far explain how well a test structure explains the experimental spectrum. Another way to define an R-factor is to look how well the simulated signals are explained (R_6). For the results shown in Table 1 α was set to $-1/6$ and again only long-range and non-assigned NOEs were used. A cut-off of 0.5 nm for the simulated signals was applied during the calculations. For both *Tm*Csp and HPr the R-factors are improving by going from the extended strand to the original structure. However, the difference in R-factors between the best and worst structure is only 0.14 and 0.18 for *Tm*Csp and HPr, respectively. In comparison to R_5 ($\alpha = -1/6$) the results obtained by R_6 ($\alpha = -1/6$) are less discriminating and the R-factors are quite high. These results can be explained by a relatively high number of simulated peaks for which no corresponding experimental peaks were found. For example, this loss of experimental peaks can be caused by fast exchanging H^N-protons and conformational flexibility. On the other hand, it could mean that the structures calculated from the assigned NOEs do not use the existing information optimally, that is, that the non-NOEs should be used for the structure calculation.

Instead of using the standard noise intensity in R_4 and R_5 it is possible to assign the non-assigned signals solely on the basis of chemical shifts and assign specific volumes to these peaks (R_7 ($\alpha = -1/6$)). To make sure that no noise or artefact signals remain in the group of unassigned signals only signals out of this group were accepted with probability values greater than 0.98. Table 1 shows the resulting R-factors for *Tm*Csp and HPr. In this case best results were obtained when all assigned and non-assigned signals were used. In general the R-factors obtained in this test case are somewhat less discriminating and larger than the R-factors obtained using R_5 ($\alpha = -1/6$). A detailed analysis of the data shows that mainly a few non-assigned peaks that correspond to large distances in the test structure are responsible for this behaviour. These are mostly artefact peaks originating for example from the water signal, that were neither removed by the lattice algorithm nor by the probability value

Table 1. Various R-factors for TmCsp and HPr

	R_2 ($\alpha = -1/6$)[a]	R_4 ($\alpha = 1$)[b]	R_4 ($\alpha = -1/6$)[b]	R_5 ($\alpha = -1/6$)[b]	R_6 ($\alpha = -1/6$)[b]	R_7 ($\alpha = -1/6$)[c]	RMSD[nm][d]
TmCsp							
Extended	0.21	0.99	0.56	0.92	0.99	0.96	3.14
Few NOEs	0.20	1.00	0.45	0.51	0.90	0.56	0.36
Homology model	0.19	0.96	0.41	0.45	0.89	0.51	0.24
Original	0.19	0.99	0.38	0.43	0.85	0.53	0.09
HPr							
Extended	0.23	0.99	0.53	0.93	0.99	0.98	3.95
MD9000	0.22	0.99	0.44	0.77	0.94	0.80	0.59
MD6000	0.21	0.98	0.39	0.59	0.89	0.74	0.37
MD3000	0.19	0.94	0.39	0.48	0.84	0.67	0.18
Original	0.16	0.83	0.39	0.44	0.81	0.62	0.11

[a]For R_2 all assigned signals were used.
[b]For R_4, R_5 and R_6 long-range and non assigned NOEs were used.
[c]When R-factors according to R_7 were calculated best results were obtained when all assigned and non assigned signals were used.
[d]The pairwise RMSD values for the Cα atoms were calculated between the original and the other test structures. The RMSD value for the original structure was obtained using a bundle of five final solution structures. In this case the average RMSD to the mean structure was calculated.

filtering. The errors introduced by these peaks increase as the volume of the structure increases. Therefore the resulting R-factors are biased by the volume of the structure. This can be dangerous, since there is no general correlation between accuracy and volume of a structure. However, this R-factor definition has the benefit that it is independent of a standard noise level. On the other hand, it has some limitations, as mentioned above.

We have investigated if there is a correlation between R-factors and RMSD values. Pair-wise RMSD values for the Cα atoms were calculated for each test set between the original and the other structures. These RMSD values should be a measure for the accuracy of a selected structure. The RMSD values for the original structure were calculated using a bundle of 5 final accepted solution structures and the average RMSD value to the mean structure was determined. This RMSD value is a measure for the precision of the original structure. Table 1 displays the corresponding R-factors and RMSD values. A correlation between RMSD value and R-factor is clearly visible as with increasing R-factors the RMSD values increase as well. The observed correlation is especially clear if R-factors were calculated using R_5 ($\alpha = -1/6$). This is in line with the expected correlation between the R-factor and the accuracy of a structure.

Discussion

The R-factor determination described here has two new aspects compared to already published work in this field, i.e. (1) the automated assignment of NOE cross peaks and (2) the definition of new forms of R-factors which include e.g. the non-assigned experimental or back-calculated peaks. The two parts are in principle independent from each other, that is, the automated routines for the cross peak assignment can be used in conjunction with any published (or to be published) definition of an R-factor. The automated assignment of the experimental spectrum is based on already published routines for automated peak picking (Neidig et al., 1990), automated integration (Geyer et al., 1995), automated signal and artefact recognition (Antz et al., 1995; Schulte et al., 1997) and the back calculation of the NOE spectra using the complete relaxation matrix formalism (Görler and Kalbitzer, 1997; Görler et al., 1999a). It assumes that the basic assignments contained in an assignment table are correct (including the stereo specific assignments) and only identifies the cross peaks on the basis of these assignments. It allows only small variations of chemical shifts contained in the chemical shift table and adapts them to the experimental spectrum. This is in contrast to other programs which try an automated assignment of cross peaks for structure calculations (for a review see Moseley and Montelione, 1999). In our case the structure is given and only its quality has to be assessed. Therefore the assignment problem concerning

the experimental cross peaks is strongly reduced but still not trivial, since overlap of cross peaks, small temperature shifts and the occurrence of non-recognised artefact (or impurity) peaks may lead to errors. However, the maximum likelihood method developed by us (Görler, 1998) works sufficiently well for this purpose. For R_7 the assignment strategy for the non-assigned peaks is similar to the assignment strategy used within the programs ARIA and NOAH (Mumenthaler et al., 1995; Nilges et al., 1997). If there are several assignment possibilities for one experimental peak ARIA uses them all. However, in the following structure calculation the possibility that corresponds to the shortest distance is weighted the most. Within NOAH all assignment possibilities are used and incorrect ones are removed by violation analysis. In our case we select the one that corresponds to the largest volume (shortest distance), which is in some regards similar to the weighting in ARIA.

Part (2) comprises the definition of R-factors which we have tested on two different proteins. From the results it is clear how dependent the obtained R-values are on the used form of the R-factor. One should select the most discriminating R-factor to have the most sensible measure for the quality of a structure. The best results in this regard are found by using R_5 ($\alpha = -1/6$) and applying it only to the long-range and non-assigned NOEs. A comparison with the results obtained using R_3 ($\alpha = -1/6$) shows the importance of the non-assigned NOEs, since the results obtained using R_3 are much less discriminating. This is true independent of the used subset of atoms (intra-residual, sequential, medium-range, long-range and inter-residual). The results displayed in Table 1 show that there is a correlation between R-factors and the accuracy of a structure. If one is interested in a more detailed analysis of a structure one can calculate separate R-factors for the various secondary structure elements (Figure 2). This should be particularly useful in the beginning of the structure calculation process when the user is interested in the quality of its starting model. One possibility is to test if the α-helices and β-strands adopt the correct length. For example, if one calculates an R-factor for a specific α-helix in the model structure the R-factor should reflect if the whole region is really α-helical. Since the R-factor calculation and with it the assignment of the NOESY spectra is automated, these calculations can be performed as soon as the sequential assignment is completed. For example, at this stage it is possible to test different model structures and to select the one with the lowest R-factors as a starting structure for the NOE assignment process. It should be noted that the concept of residue specific R-factors as displayed in Figure 3 has been used previously (Edmondson et al., 1995). However, Figure 3 shows for HPr a good example how R-factors might be used as a tool to investigate the dynamics of proteins. This might be particularly useful in cases where no ^{15}N labelling is available and the standard ^{15}N T_1, T_2 and ^1H-^{15}N hetero NOE measurements cannot be performed. Figure 3 clearly shows that a rigid sphere model which was assumed for the back calculation of the NOEs is not correct for all parts of the HPr molecule, while it explains the *Tm*Csp structure fairly well. For HPr especially the terminal ends seem to be quite flexible. In Figure 4 R-factors were grouped into distance classes. This figure gives an indication how important the NOE upper bounds can be for the structure calculations, especially for short and long distances. We have tried to find different R-factor definitions that do not use a 'standard' noise level (R_3 and R_7). However, the results obtained using one of these equations proved to be less satisfactory for calculating an R-factor for the whole molecule. When using these factors generally the same trends were observed as with R_5. However, R_5 gave by far the most structurally sensitive R-factors. R_6 defines an R-factor that explains how well the back calculated signals are explained. The results show that this R-factor definition is very sensitive to the completeness of the experimental spectrum. For example, missing experimental peaks due to solvent or conformational exchange will lead to an increase of the R-factor. A comparison of the results obtained using R_5 and a previously published R-factor R_2 ($\alpha = -1/6$) (Gonzalez et al., 1991) clearly shows that our R-factor definition is more sensitive to structural differences and is therefore well suited to judge the quality of a protein structure.

In summary, R_5 is best suited for a general definition of the R-factor while R_3 is well suited for local R-factors. In all R-factors used, the coefficient $\alpha = -1/6$, that also has been previously used for R-factor definitions (Gonzalez et al., 1991; Thomas et al., 1991; Brünger et al., 1993; Clore et al., 1993), is superior to $\alpha = 1$. The R-factor program RFAC should be a useful tool for assessing the quality of a structure. Although tested here on protein structures, it can be applied to any macromolecular structure. Since the whole process is automated, different structures can be compared in a very fast manner.

Acknowledgements

We like to thank M. Geyer and S. Harrieder for their help with the assignment of the *Tm*Csp protein and T. Maurer for helpful discussions. We thank B. Schuler and R. Jaenicke for providing the *Tm*Csp and W. Hengstenberg for providing HPr. This work was supported by the Deutsche Forschungsgemeinschaft (W.G., H.R.K.) and the Biotechnology Program of the European Union (H.R.K.).

References

Antz, C., Neidig, K.-P. and Kalbitzer, H.R. (1995) *J. Biomol. NMR*, **5**, 287–296.

Baleja, J.D., Moult, J. and Sykes, B.D. (1990) *J. Magn. Reson.*, **87**, 375–384.

Beneicke, W. (1994) Ph.D. Thesis, University of Heidelberg, Heidelberg.

Bonvin, A.M.J.J., Boelens, R. and Kaptein, R. (1991) *J. Biomol. NMR*, **1**, 305–309.

Borgias, B.A., Gochin, M., Kerwood, D.J. and James, T.L. (1990a) *Prog. NMR Spectrosc.*, **22**, 83–100.

Borgias, B.A. and James, T.L. (1990b) *J. Magn. Reson.*, **87**, 475–487.

Brünger, A.T., Campbell, R.L., Clore, G.M., Gronenborn, A.M., Karplus, M., Petsko, G.A. and Teeter, M.M. (1987) *Science*, **235**, 1049–1053.

Brünger, A.T., Clore, G.M., Gronenborn, A.M., Saffrich, R. and Nilges, M. (1993) *Science*, **261**, 328–331.

Clore, G.M., Robien, M.A. and Gronenborn, A.M. (1993) *J. Mol. Biol.*, **231**, 82–102.

Cullinan, D., Korobka, A., Grollman, A.P., Patel, D.J., Eisenberg, M. and Santos, C. (1996) *Biochemistry*, **35**, 13319–13327.

Edmondson, S.P., Lingshi, Q. and Shriver, J.W. (1995) *Biochemistry*, **34**, 13289–13304.

Ferrige, A.G. and Lindon, J.C. (1978) *J. Magn. Reson.*, **31**, 337–340.

Geyer, M., Neidig, K.-P. and Kalbitzer, H.R. (1995) *J. Magn. Reson.*, **B109**, 31–38.

Gonzalez, C., Rullmann, J.A.C., Bonvin, A.M.J.J., Boelens, R. and Kaptein, R. (1991) *J. Magn. Reson.*, **91**, 659–664.

Görler, A. (1998) Ph.D. Thesis, University of Heidelberg, Heidelberg.

Görler, A. and Kalbitzer, H.R. (1997) *J. Magn. Reson.*, **124**, 177–188.

Görler, A., Gronwald, W., Neidig, K.-P. and Kalbitzer, H.R. (1999a) *J. Magn. Reson.*, **137**, 39–45.

Görler, A., Hengstenberg, W., Kravanja, M., Beneicke, W. and Kalbitzer, H.R. (1999b) *Appl. Magn. Reson.*, **17**, 465–480.

Gupta, G., Sarma, M.H. and Sarma, R.H. (1988) *Biochemistry*, **27**, 7909–7919.

Harrieder, S. (1998) Diploma Thesis, University of Regensburg, Regensburg.

Jeener, J., Meier, B.H., Bachmann, P. and Ernst, R.R. (1979) *J. Chem. Phys.*, **71**, 4546–4553.

Kremer, W., Harrieder, S., Geyer, M., Gronwald, W., Welker, C., Jaenicke, R. and Kalbitzer, H.R. (2000) *Protein Sci.*, submitted.

Lane, A.N. (1990) *Biochim. Biophys. Acta*, **1049**, 189–204.

Laskowski, R.A., MacArthur, M.W. and Thornton, J.M. (1998) *Curr. Opin. Struct. Biol.*, **8**, 631–639.

Lefevre, J.-F., Lane, A.N. and Jardetzky, O. (1987) *Biochemistry*, **26**, 5076–5090.

Marion, D. and Wüthrich, K. (1983) *Biochem. Biophys. Res. Commun.*, **113**, 967–974.

Mertz, J.E., Güntert, P., Wüthrich, K. and Braun, W. (1991) *J. Biomol. NMR*, **1**, 247–248.

Moseley, H.N.B. and Montelione, G.T. (1999) *Curr. Opin. Struct. Biol.*, **9**, 635–642.

Mumenthaler, C. and Braun, W. (1995) *J. Mol. Biol.*, **254**, 465–480.

Neidig, K.-P., Saffrich, R., Lorenz, M. and Kalbitzer, H.R. (1990) *J. Magn. Reson.*, **89**, 543–552.

Neidig, K.-P., Geyer, M., Görler, A., Antz, A., Saffrich, A., Beneicke, W. and Kalbitzer, H.R. (1995) *J. Biomol. NMR*, **6**, 255–270.

Nikonowicz, E.P., Meadows, R.P. and Gorenstein, D.G. (1990) *Biochemistry*, **29**, 4193–4204.

Nilges, M., Habazettl, J., Brünger, A.T. and Holak, T.A. (1991) *J. Mol. Biol.*, **219**, 499–510.

Nilges, M., Macias, M.J., O'Donoghue, S.I. and Oschkinat, H. (1997) *J. Mol. Biol.*, **269**, 408–422.

Schulte, A.C., Görler, A., Antz, C., Neidig, K.-P. and Kalbitzer, H.R. (1997) *J. Magn. Reson.*, **129**, 165–172.

Thomas, P.D., Basus, V.J. and James, T.L. (1991) *Proc. Natl. Acad. Sci. USA*, **88**, 1237–1241.

Welker, C., Böhm, G., Schurig, H. and Jaenicke, R. (1999) *Protein Sci.*, **8**, 394–403.

Xu, Y., Sugar, I.P. and Krishna, R. (1995) *J. Biomol. NMR*, **5**, 37–48.